Research Article

The effect of copper on the multiple carbon nanofilaments growths by the methane decomposition over the oxidized diamond-supported nickel–copper bimetallic catalyst

M. Shiraishi[1,2] · K. Nakagawa[2,3] · T. Ando[2,4] · M. Nishitani-Gamo[2,5]

© The Author(s) 2022   OPEN

Abstract

To clarify the indispensable parameters for the multiple carbon nanofilaments (CNFs) growths, in other words, having a unique Octopus-like morphology consisting of the Marimo-like carbon (MC), we have systematically studied to synthesize the MC by the decomposition of methane using oxidized diamond-supported Ni–Cu bimetallic catalysts. We discovered that a Cu addition of 20 wt.% by weight and a growth temperature in the region of 550 °C to 600 °C resulted in many CNF forms from a single catalyst particle, specifically the "Octopus-like" morphology of CNFs. We also discovered that the several CNFs forms might occur from the carbon dissolved in the sintered catalyst particles. We described a model process of the unique structure formation. We expect that the Octopus-like CNFs growth gives enough space volume in the MC for a mass transfer, consequently, it should contribute to realizing a higher power generation performance of a polymer electrolyte fuel cell (PEFC) although under a higher-voltage generation region.

Keywords Marimo-like carbon · Nickel · Copper · Bimetallic catalyst · Carbon nanofilament · "Octopus-like" morphology

1 Introduction

Fibrous carbon nanoparticles were discovered by electron microscopy over 70 years ago and described as "an unusual form of carbon" generated by the catalytic reaction of carbon monoxide over iron oxide tiny particles included in a brick [1]. At that time, another transition metals of cobalt and nickel were also used as a catalyst for growing carbon filaments [2]. It is now known as a carbon nanofiber or nanofilament; this type of carbon represents a unique quality, such as high surface area and high electrical conductivity at the same time. Many trials for generating vapor–grown carbon nanofiber catalyzed hydrocarbons over small metal particles began in the 1970s and 1980s

[3–7]. A simultaneous yield of hydrogen and fibrous carbon nanomaterials has again attracted the attention of researchers working on the catalytic decomposition of methane over Ni catalysts [8]. To realize structure-controlled fibrous carbon nanomaterials growth, a role of catalyst metal particles is essential, and this concept has been widely accepted in the research field by the pioneered studies reviewed in Ref. [9]. As a result of the potential for various applications, a somewhat large–scale process involving the catalytic decomposition of hydrocarbons over tiny metal particles has been extensively studied.

To tune the catalyst reactivity, some research groups have been focused on the effect of bimetallic, especially Ni and Ni-based by the addition of Cu as catalysts for the

✉ M. Nishitani-Gamo, mngamo@toyo.jp | ¹Graduate School of Science and Engineering, Course of Applied Chemistry, Toyo University, Saitama, Japan. ²Research Institute of Industrial Technology, Toyo University, Saitama, Japan. ³Department of Chemical Engineering, Kansai University, Osaka, Japan. ⁴National Institute for Materials Science (NIMS), Ibaraki, Japan. ⁵Department of Applied Chemistry, Toyo University, Saitama, Japan.

production of carbon nanostructures [10–13]. Nishiyama and co-workers [10] reported that the addition of Cu on Ni promoted the catalytic activity for carbon formation, and also found that the Ni–Cu–particle diameter was larger than the fiber diameter formed on metals of higher Cu content. The SEM image of the fibrous material revealed that one metal particle generated two or three fibers. Bernardo and associates [11] discovered similar SEM photos of the shape of carbon generated by the decomposition of methane over a silica-supported Ni–Cu catalyst and referred to it as "octopus" carbon. Rodriguez, Baker, and colleagues conducted extensive research on the effect of Cu addition to Fe [14], Co [15], and Ni metals on carbon nanostructures and determined that Cu–Ni alloys were the most effective catalysts for the reaction. In the periodic table of the elements, Cu is next to Ni, however, their chemical nature is different; Ni can catalyze hydrocarbons and indicate a higher carbon solubility, while Cu cannot [2, 16, 17]. Although Cu itself does not catalyze hydrocarbons to form carbon nanofilaments, Cu addition to Ni enhances the activity to decompose and form carbon nanofilaments. The Ni-based Cu bimetallic catalyst is both attractive and important for studying growth mechanisms and realizing an acceptable procedure for several applications.

We have developed and studied to grow a novel spherical carbon [18], we named it the 'Marimo-like carbon' (abbreviated as MC) after its spherical shape looks like the 'Marimo' which is algae lived in Lake Akan of Hokkaido. The fundamental particle of MC is a carbon nanofilament (CNF), and a large number of CNF cluster to generate its spherical shape. The greater graphitized CNFs are obtained by a decomposition of hydrocarbons, particularly methane, over an oxidized-diamond supported Ni catalyst. We have interested in this higher activity of Ni catalyst loaded on the oxidized-diamond support for CNFs deposition [19]. The oxidized-diamond surface shows a specific electronic structure as it is chemisorbed with oxygen-included functional groups, otherwise, the diamond bulk is an insulator and electrons are strictly localized at the chemical bond. The oxidized-diamond surface is expected to act as solid carbon oxide material, and to affect the electronic states of supported metal particles related to its catalytic activity. The MC includes diamonds as a core; the MC is all-carbon material, in other words, a sp^2-sp^3 carbon composite. We have proposed the MC as the Pt catalyst support for use in the polymer electrolyte fuel cell (PEFC) catalyst layer and proved that the membrane electrode assembly using Pt/MC (MC-MEA) needed less ionomer to keep a form of cathode catalyst layer [20], consequently, the MC-MEA efficiently worked in the high current density range compared to an existing catalyst using amorphous carbon. Because the MC has a space volume between the CNFs, the reactant gas and product water could readily pass through the space volume [21]. The accelerated deterioration test (ADT) revealed that the MC was a more oxidation-resistant support than ordinary carbon black [22]. This result indicates that the sp^2-crystallinity of CNF is much higher compared to the carbon black. To realize a high-performance PEFC, the catalyst support carbon material should be a higher-ordered fibrous structure, and keep an appropriate space volume between fibers. It is essential to control both the CNF sp^2-structure and the space volume between CNFs.

In this study, we investigated intensively the synthesis of MC by the decomposition of methane using oxidized diamond-supported Ni–Cu bimetallic catalysts in order to clarify the effect of Cu addition on the morphology and fine structure of CNF. We discovered that regulated Cu addition resulted in the formation of many CNFs from a single catalyst particle, specifically the "Octopus-like" morphology of CNFs. We described a model process for the development of a unique structure.

2 Experimental

The oxidized diamond powder (diamond powder: SANDVIK HYPERION, Worthington, OH in USA, Type RVM 0–0.5) calcined at 450 °C in the air was used as catalyst support. The MC growth catalyst was prepared by impregnating it with a mixed aqueous solution of nickel nitrate hexahydrate and copper nitrate trihydrate (special grade, FUJIFILM Wako Pure Chemical Corporation, Osaka, Japan). The solution contained in the diamond powder was dried before being calcined in the air at 400 °C. The oxidized diamond powder loaded with 5wt.% Ni–Cu–catalyst is referred to Ni–Cu–(5 wt.%)/O-dia. The growth conditions for the MC are shown in Table 1. We used a fixed-bed type quartz reactor (GEN-TECH, INC., Yokohama, Japan) for the growth experiments. Methane was used as the reaction gas and the flow rate was set at 30 sccm. The bimetal catalyst used for the MC growth was Ni–Cu–(5 wt.%)/O-dia. with the copper concentration in the range from 0 to 90 wt.%. The growth temperature was in the range of 400 to 725 °C to investigate the effect of the temperature on the CNF morphology. To understand the initial stage of the growth process, the duration time was in the range from 0 to 4 h.

Table 1 MC growth condition

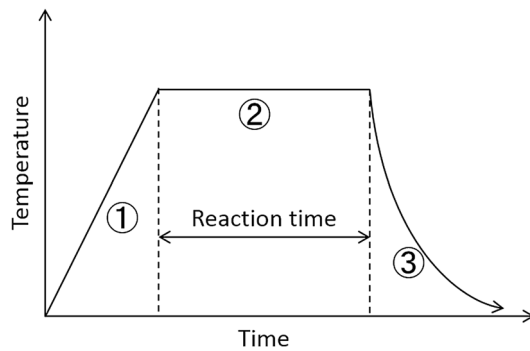| Catalysts	Ni-Cu(5wt.%) / O-dia. (100 mg)
	Cu ratio: 0–90%
Reaction temperature	400~725 °C
Reaction time	0~4 h
Reaction gas	CH$_4$
Flow rate	30 sccm
Space Velocity	18,000 mL (1 h. g-cat.)$^{-1}$

Fig. 1 The growth steps of the Marimo-like carbon. Step 1: Heating-up period. The catalyst was brought into the reactor on a quartz boat, then heated to the appropriate temperatures in the Ar gas flow. The rate of temperature rise was 20 K/min. Step 2: Catalytic reaction period. The Ar gas was changed to methane for the Marimo-like carbon growth. Step 3: A period of rest is required. When the growth process was completed, the heating power supply was turned off, and the methane gas flow was converted to the Ar gas flow to cool the grown material to room temperature
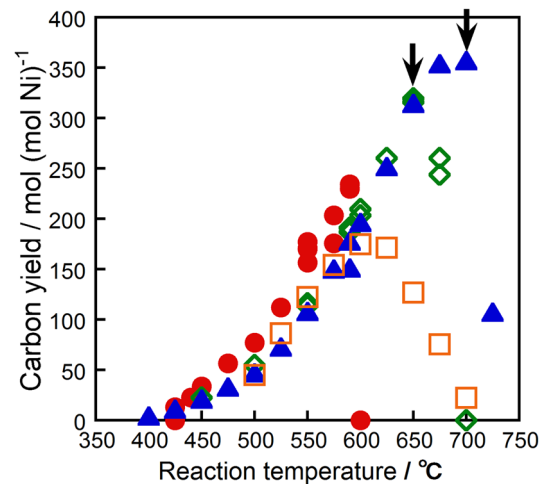

Fig. 2 The relation between the reaction temperature and the carbon yield of the Marimo-like carbon growth using the Ni–Cu–bimetal catalyst with the Cu ratio of 0% (solid circle mark), 20% (open rhombus mark), 50% (solid rectangular mark), and 90% (open square mark), respectively

The MC formation was carried out in three steps, as indicated in Fig. 1. Step 1 was the temperature raising time; the catalyst was placed in the reaction tube and electrically heated to the reaction temperature in the Ar gas flow at a rate of 20 K/min. The catalytic reaction period was the second step. The reaction temperature was kept constant, and methane gas was injected before turning off the Ar gas flow. In this study, we defined step 2 as the reaction period. Step 3 is the post-reaction process, a cooling-down duration. As the growth process was finished, the heating power supply was off and the methane gas flow was switched to the Ar gas flow to cool down the MC to a room temperature. The amount of grown CNFs was calculated from a weight gain yielded by the growth process.

Scanning electron microscopy (SEM; S-4100, Hitachi High-Tech Corporation, Tokyo, Japan) was used to examine the morphology and nanostructure of the obtained MC. A variation of the earliest step of the CNFs development phase was revealed using transmission electron microscopy (TEM; JEM-2100, JEOL Ltd.).

3 Results and discussion

3.1 The Effect of Cu addition in the Ni–Cu–bimetal catalyst on the MC growth

Figure 2 shows the relation between the reaction temperature and the amount of carbon deposition by using the Ni–Cu–catalyst having various Cu concentrations. No carbon deposition was obtained by the catalytic reaction of methane over the Cu/O-dia. catalyst. As the Ni/O-dia.

catalyst was used for MC growth, and the reaction temperature of 590 °C resulted in the most carbon deposition, as demonstrated by the solid circle mark. There was no carbon deposition at 600 °C, which was only 10 °C higher than 590 °C. According to the X-ray photoelectron spectra [18], Nakagawa et al. showed that the supported Ni particles may diffuse into the oxidized diamond support under at a higher temperature of 600 °C. Under the reaction temperature of 600 °C, the supported Ni catalysts were hidden under the diamond surface, consequently, methane could not catalytically react with Ni resulted in no carbon yield.

We found that the temperature giving the maximum amount of carbon yield shifted to a higher temperature over 590 °C by the addition of Cu to the Ni catalyst. As indicated by the left arrow in Fig. 2, the Ni–Cu bimetal catalyst containing 20% Cu (we briefly explained it as 'Ni8-Cu2/O-dia.', indicated by an open rhombus mark) was used for the growth, and the maximum carbon deposition temperature was 650 °C, which is 60 °C higher than the 590 °C observed when using the Ni/O-dia. catalyst. When Ni5-Cu5/O-dia. was used for the growth (solid rectangular mark), as indicated with the right arrow in Fig. 2, the maximum carbon yield temperature shifted to the further high-temperature around at 700 °C. We speculate that the existence of Cu in the bimetal catalyst could play a role in preventing the Ni diffusion into the diamond support, which was observed at the reaction temperature of 600 °C with using Ni/O-dia. catalyst.

As shown in Fig. 2, when 20% wt Cu was added to the Ni catalyst, the maximum carbon deposition increased from 229.8 mol Ni-mol^{-1} produced using the Ni/O-dia.

catalyst to 319.7 mol Ni-mol^{-1}. The quantity of maximum carbon deposition obtained using Ni5-Cu5/O-dia. catalyst was 357.0 mol Ni-mol^{-1}; this amount of carbon deposition was 1.55 times greater than that obtained using Ni/O-dia. catalyst. This tendency is consistent with both the result studied by Nishiyama et. al. [10] for benzene decomposition on the Cu-Ni alloy sheets and that of reported by Ashok et al. [23] for the decomposition of methane on a SiO$_2$-supported Ni–Cu–catalyst. Nishiyama et. al. reported that the increase of carbon deposition by the addition of Cu would be yielded by the preventing effect of Cu on the Ni surface coverage with a carbon layer. They proposed that Cu-atoms partially dominated the surface of the catalyst particle, implying that the Ni–Cu–surface composition was not uniform. As the catalytic reaction sites, a Ni-rich patch on the catalyst particle surface might react with the gas molecules. The presence of Cu in the catalyst particle is expected to boost the reactivity of the Ni-rich region to the decomposition of gas molecules. Ashok et al. [23] also supported the lack of uniformity of the catalyst particle composition; it consisted of a Ni-rich area and a Cu-rich area, and the latter was known as having a higher affinity with the graphite structure. As a result, a Cu-rich area would limit the formation of a graphite layer on the Ni-rich surface, and the reactivity of the Ni-rich area could be preserved and aided in the synthesis of solid carbon. Although the details of the effect of Cu addition to the Ni catalyst on the increase of a maximum carbon yield and a higher shift of its temperature, the existence of a Ni-rich area and a Cu-rich area in the Ni–Cu–catalyst, such an inhomogeneous structure would be essential for increasing the reactivity of Ni to solid carbon deposition, are unknown.

Figure 3 shows the amount of the carbon yield per 1 mol of Ni as a function of Cu content in the Ni–Cu bimetal catalyst under different reaction temperatures. In the case of the reaction temperature of 550 °C (solid circle mark), the carbon yield decreased with an increase of Cu content in the range from 0 to 20 wt.%. As the Cu content is above 20 wt.%, the carbon yields per 1 mol of Ni almost kept constant although the Cu content increased. Carbon yields decreased with a rise in Cu content in the range from 5 wt.% to 20 wt.% in the case of the reaction temperature of 600 °C (solid rohmbus mark) then appeared to be constant above 20 wt.% Cu, as observed in the case of 550 °C growth. At a higher temperature of 650 °C (open rectangular mark), a catalyst containing 10% Cu resulted in no carbon deposition. In contrast, raising the Cu concentration from 15 to 50% resulted in a significant increase in carbon yields. The Cu content above 20 wt.% gave a small effect to the amount of carbon deposition compared to that observed below the 20 wt.% Cu. This indicates that the reactivity of Ni–Cu–catalyst below or above 20 wt.%
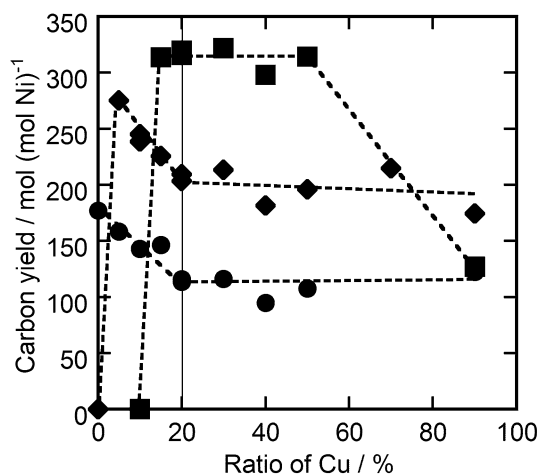
Fig. 3 The effect of Cu addition in the Ni-Cu bimetal catalyst on the carbon yield under various reaction temperatures of 550 °C (solid circle mark), 600 °C (solid rhombus mark), and 650 °C (solid square mark), respectively

Cu content is suggested to be through different mechanisms. We focused on the effect of 20 wt.% Cu content on the MC growth.

There was no carbon deposition with 100% Ni at the reaction temperature of 600 °C, and a modest amount of Cu addition greatly increased the carbon yield. Because Ni particles on the diamond support could be dissolved into the diamond above 600 °C in our system, no carbon deposition occurred above 600 °C. We speculate that a small amount of 5 wt.% Cu addition can play a role at the bimetal catalyst particle surface for preventing Ni from dissolving into the diamond support. It is expected that the Ni–Cu–catalyst particle supported on the diamond has a Cu-rich surface; It would prevent Ni–Cu–catalyst particles from dissolving into the diamond support at temperatures above 600 °C, and as a result, Ni–Cu–catalyst might result in carbon deposition. These experimental results also indicated the existence of a Cu-rich patch on the Ni–Cu–catalyst surface, as well as an inhomogeneous structure of Ni–Cu–particles.

3.2 The effect of Cu addition in the Ni–Cu–bimetal catalyst on the multiple-CNFs formation from one catalyst particle

Figure 4 shows SEM images of the MCs grown using different Cu contents catalysts under three-kinds of reaction temperatures. Fibrous carbon nanomaterials were observed and any other form of carbon such as amorphous carbons could not. As indicated in the SEM images with arrowheads, we found that multiple CNFs grow from one catalyst particle likely as an "octopus". To clarify the growth conditions that resulted in an octopus-like morphology, 50
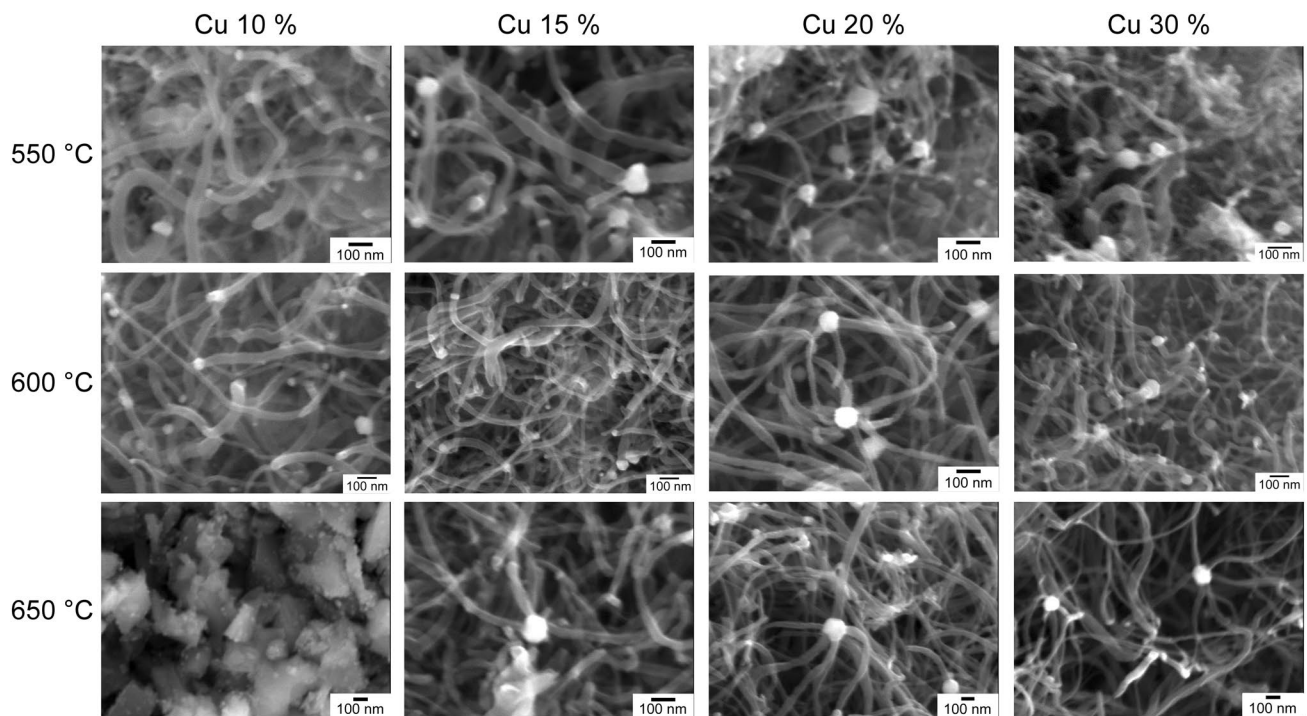
Fig. 4 SEM images of the Marimo-like carbon grown with Ni-Cu bimetal catalysts

to 150 over catalyst particles were analyzed to count the number of CNFs generated from the particles using SEM images. Because a CNF was formed from a single catalyst particle, its morphology was classified as "1". Two CNFs were grown from one particle was named "2". In the same way, three CNFs were grown from one particle was "3". We counted how many particles as called "1", "2", "3", "4", and "5", then made histograms of the distribution of the five types of catalyst particles, as shown in Fig. 5. In the case of the 10 wt.% Cu content, the ratio of "1" and "2" particles were over 60% in the counted particles. As the Cu content of 15 wt.%, 550 °C growth gave a distribution peak at "2". When the temperature was raised to 600 °C, 40% of the catalyst particles produced one CNF growth, as shown by a peak at "1". The histogram displayed a flat distribution during higher temperature growth of 650 °C. Cu content less than 15% resulted in a slow-growing octopus-like shape. 650 °C growth produced a flat distribution regardless of Cu content. In the red-framed histograms generated from the Cu concentration of 20 wt.%, two peaks were identified at "4" and "5". With an increase of Cu content to 30 wt.%, the ratio of "5" particles grown at 550 °C decreased, and also the distribution became flat grown at 600 °C. The addition of 20% Cu to the Ni–Cu–catalyst had a significant effect on the formation of an octopus-like shape. As illustrated in Fig. 3, we discovered that the effect of Cu on carbon yields varied depending on the boundary of the 20 wt.% Cu concentration. The 20 wt.% Cu content of the

Ni–Cu–catalyst would play a crucial role in the numerous CNF development mechanisms.

To understand the multiple-CNF growth, the octopus-like morphology change was observed by FESEM during the catalytic reaction with methane using Ni8Cu2/O-dia. catalyst at the temperature of 600 °C. Figure 6 shows a morphology of the CNFs grown with a reaction time of 10 min., 30 min., and 60 min., respectively. As shown in Fig. 6(a), in the case of just 10 min. growth, catalyst particles with a shorter CNFs in the length of a sub-micron meter were grown and two-CNFs growth from one catalyst particle was occasionally observed. In the case of 30 min. In Fig. 6(b), the majority of CNFs were formed from a single catalyst particle, and a numerous CNFs were rarely observed to grow. In contrast to these occurrences, as shown in Fig. 6 (c) of a 60–min–growth, we often identified a four or five-CNFs growth from a single catalyst particle, and such multiple CNFs growths were produced. The diameter of these catalyst particles appeared to be greater than 60 nm, which was larger than the diameter of catalyst particles obtained by a shorter growing time. The observed morphological changes in Fig. 6 were consistently indicated by the histograms in Fig. 7. Figure 7 shows the histograms obtained from the SEM images in Fig. 6. Both in Fig. 7 (a) and (b), above three-CNFs growth from one catalyst particle were hardly observed. As shown in Fig. 7 (c), in the case of growth duration was 60 min., the frequency of a four or five-CNFs growth from one catalyst
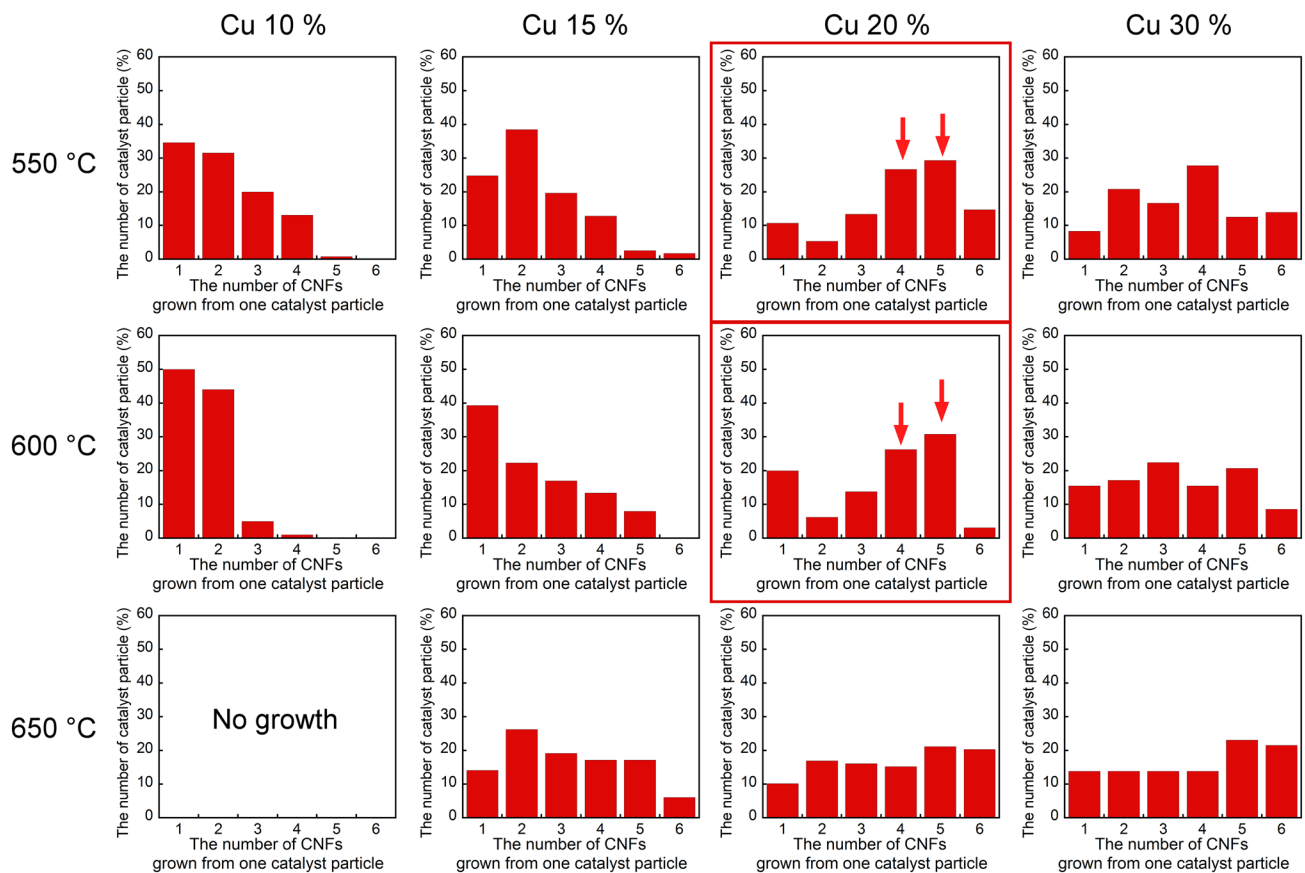
Fig. 5 The distributions of the number of CNFs grown from each of the catalyst particles counted using SEM images

particle was almost 50%. The frequency of multiple CNFs growths increased, as the growth phase increased, and the diameter of the catalyst particles appeared to be greater at the same time. Based on the FESEM data, we hypothesize that a bigger catalyst particle resulted in several CNFs growths.

To clarify the relationship between a catalyst diameter and the multiple-CNFs growth, we also observed the MC shown in Fig. 6 by using TEM. Figure 8 shows TEM images observed from the MC grown at 600 °C with using Ni8Cu2/O-dia. catalyst by a growth durations is (a) 0 min., (b) 10 min, (c) 30 min, and (d) 60 min respectively. The 0 min. reaction in Fig. 8 (a) means the heating was off at the end of Step I in Fig. 1, then cooling down in Ar flow. Figure 8(a) shows that the catalyst particle diameter was less than 10 nm. In the instance of Fig. 8(b), the diameter was less than 30 nm, and several CNFs growths were unusual. In the event of growth durations of more than 30 min., as illustrated in Fig. 8 (c) and (d), the diameter was close to 100 nm, and multiple-CNFs growth was obtained. TEM observation suggested that the catalyst diameter which gave multiple CNFs growths was larger than that observed in the case of shorter growth duration. We speculate that

an increase of the catalyst diameter during MC growth in the methane flow is a necessary step to occur the multiple CNFs growths from a single catalyst particle.

A histogram was generated from the TEM images presented in Fig. 8 to quantitatively indicate the link between the catalyst diameter and the growth of multiple-CNFs. The histograms produced from the TEM images in Fig. 8 are shown in Fig. 9. The frequency of the catalyst diameter above 60 nm increased as the growth duration increased from 0 to 60 min, as illustrated by the red rectangle area. This tendency indicates that the catalyst diameter increased with increasing of growth duration, in other words, catalytic decomposition of methane gave carbon dissolution in the Ni–Cu–catalyst particles; and resulted in growing catalyst diameter. Carbons dissolved in the catalyst particles are expected to reduce the melting temperature of Ni–Cu–particles, as a result, sintering of the catalyst particles was promoted and the diameter increased. It appears plausible to believe that four or five CNFs formed from a single catalyst particle, and that such multiple-CNFs growth occurred from sintered Ni–Cu–catalyst particles. The existence of a Cu-rich area on the Ni–Cu–catalyst surface was supported by experimental data, namely the
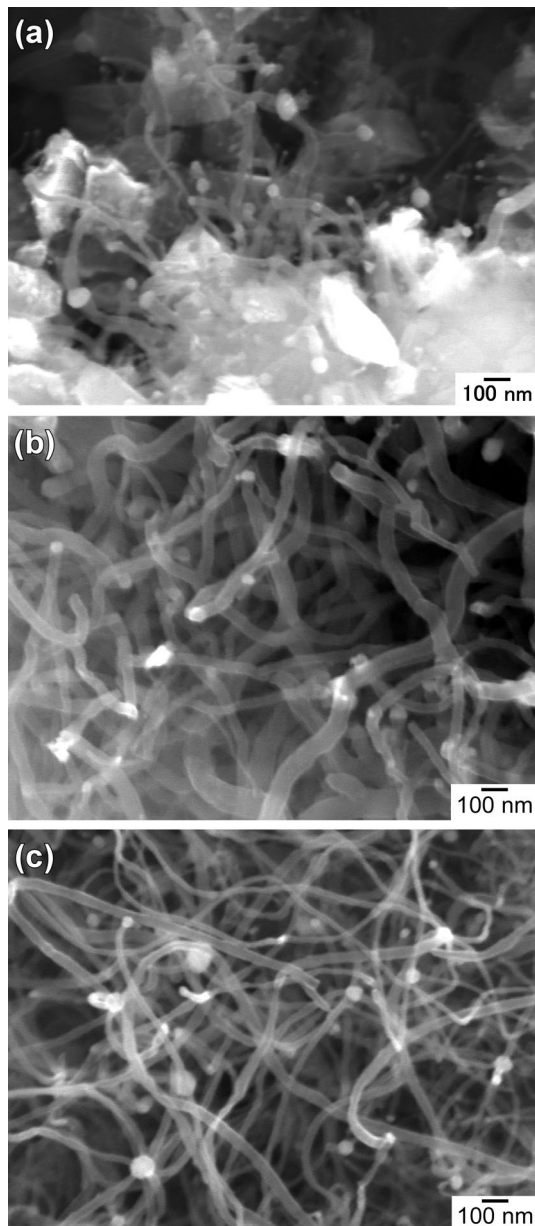
Fig. 6 The effect of reaction time on the number of CNFs produced by each catalyst particle. At a reaction temperature 600 °C, the Ni8Cu2/O-dia. was used as a catalyst. The reaction times are (a) 10 min (b) 30 min and (c) 60 min
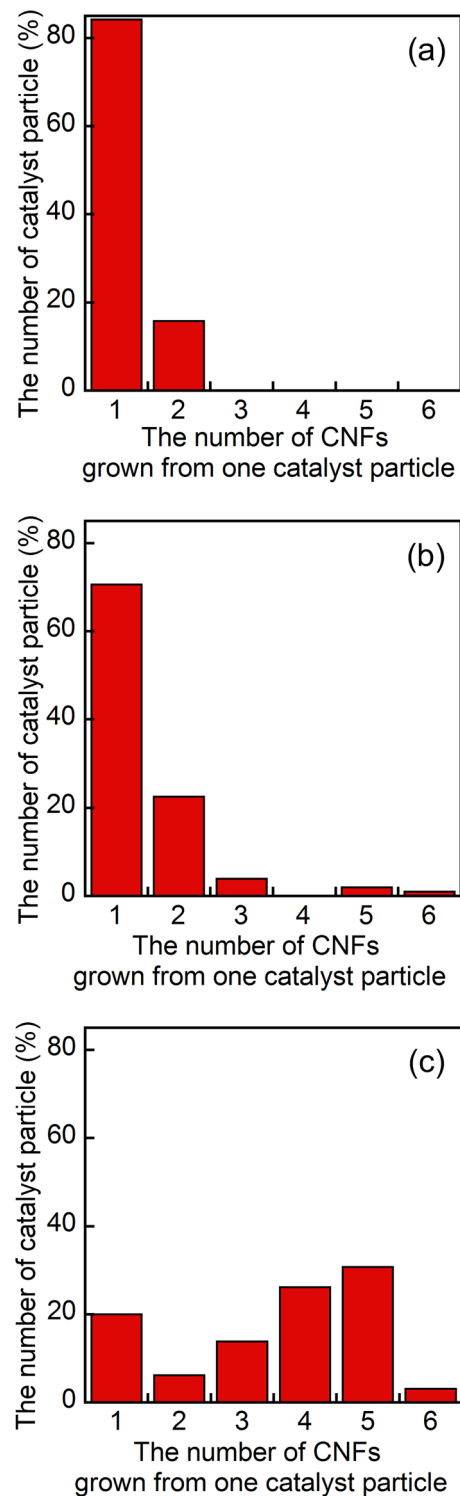

Fig. 7 The histograms were obtained from the SEM images in Fig. 6. Ni8Cu2/O-dia. catalysts were used and grown at the temperature of 600 °C. The growth duration is **a** 10 min, **b** 30 min, and **c** 60 min respectively
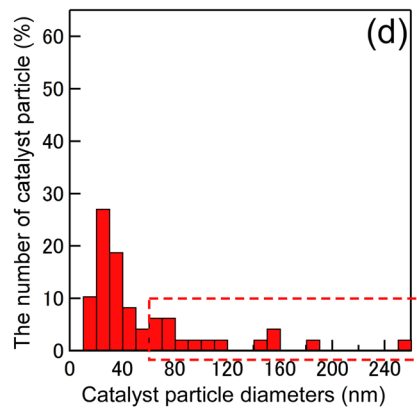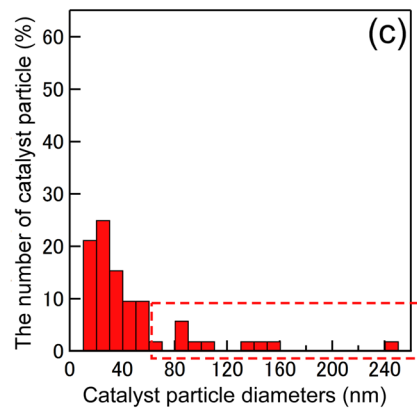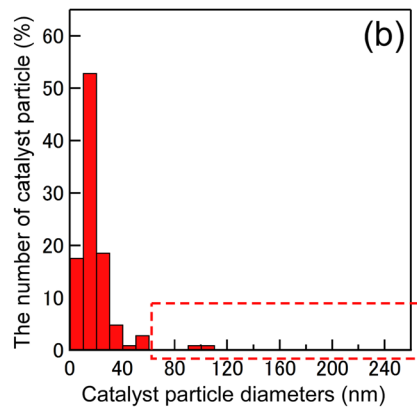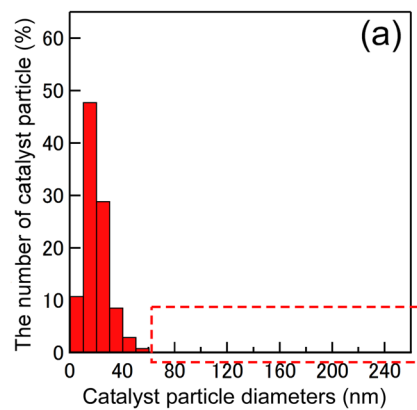
impact of Cu addition on the protection against Ni dissolution in the diamond support, as detailed in the previous section. We speculate that the sintered particle having a Cu-rich surface, in other words, a partially covered surface with Cu, resulted in the multiple-CNFs growth. In Fig. 10, we suggest a model of the multiple-CNFs growth using Ni–Cu/O-dia. catalysts. Carbons dissolved in the Ni–Cu–catalyst particles supported on the oxidized diamond were sintered as the growth period progressed. The presence of a Cu-rich area on the Ni–Cu–catalyst particle

Fig. 8 TEM images obtained from Marimo-like carbon produced at 600 °C using a Ni8Cu2/O-dia. catalyst with reaction times of (**a**) 0 min. (= heating off at the end of Step I, then cooling down in Ar flow), (**b**) 10 min., (**c**) 30 min., and (**d**) 60 min., respectively

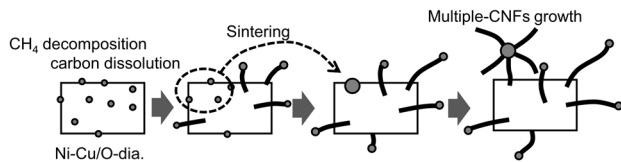◄ **Fig. 9** The histograms of the Ni8Cu2/O-dia. catalyst particle diameters measured from the TEM images. These catalyst particles were generated at 600 °C for (**a**) 0 min (=heating off at the end of Step I, then cooling down in Ar flow), (**b**) 10 min, (**c**) 30 min, and (**d**) 60 min, respectively

Fig. 10 A model of the multiple-CNFs growth using Ni–Cu/O-dia. catalyst

surface, in other words, the presence of a Ni-rich area; several CNFs growths could occur over the Ni–Cu–catalysts' Ni-rich areas.

3.3 Summary

For the multiple-CNFs growth, we experimentally revealed the necessary conditions by the systematic study. The Cu content in the Ni–Cu–bimetal catalyst was 20 wt.%. It has been proposed that the composition of Ni–Cu–particles is inhomogeneous. The Ni–Cu–catalyst particle may have a Cu-rich surface. The Ni–Cu–catalyst particle diameter was at least 60 nm or above in size could yield multiple growths. The reaction temperature ranged from 550 °C to 600 °C.

The regulated multiple-CNFs growth is projected to result in the formation of a controlled-space volume by the CNFs. The space volume provided in the MC is critical for both helping gas diffusion and a redox producing water removal [21]. We expect that the space-controlled growth process of MC will contribute to realizing a higher power generation performance although under a region of a higher-voltage generation. We are going to fabricate a membrane electrode assembly using the MC consisted with the Octopus-like CNFs as the catalyst support for the PEFC electrode.

a structure-controlled MC growth process not only to achieve higher performance of PEFC but also to explore various applications.

Declarations

References

1. Davis WR, Slawson RJ, Rigby GR (1953) An unusual form of carbon. Nature 171:756
2. Hofer LJE, Sterling E, McCartney JT (1955) Structure of the carbon deposited from carbon monoxide on iron, cobalt and nickel. J Phys Chem 59:1153–1155
3. Koyama T (1972) Formation of carbon fibers from benzene. Carbon 10:757–758
4. Koyama T, Endo M, Onuma Y (1972) Carbon fibers obtained by thermal decomposition of vaporized hydrocarbon. Jpn J Appl Phys 11:445–449
5. Endo M, Yamanashi H, Doll GL, Dresselhaus MS (1988) Preparation and electrical properties of bromine intercalated vapor-grown carbon fibers. J Appl Phys 64:2995–3004
6. Tibbetts GG (1983) Carbon fibers produced by pyrolysis of natural gas in stainless steel tubes. Appl Phys Lett 42:666–668
7. Benissad F, Gadelle P, Coulon M, Bonnetain L (1988) Formation de fibres de carbone a partir du methane: I croissance catalytique et epaississement pyrolytique. Carbon 26:61–69
8. Hamza Fakeeha A, Sadeq Al-Fatesh A, Aidid Ibrahim A, ElhagAbasaeed A (2021) CO_2 reforming of CH_4 over Ni-catalyst supported on yttria stabilized zirconia. J. Saudi Chem. Soc. 25:101244–101252
9. Rodriguez NM (1993) A review of catalytically grown carbon nanofibers. J Mater Res 8:3233–3250
10. Nishiyama Y, Tamai Y (1974) Carbon formation on copper-nickel alloys from benzene. J Catal 33:98–107
11. Bernardo CA, Alstrup I, Rostrup-Nielsen JR (1985) Carbon deposition and methane steam reforming on silica-supported Ni-Cu catalysts. J Catal 96:517–534
12. Kim MS, Rodrigues NM, Baker RTK (1991) The interaction of hydrocarbons with copper-nickel and nickel in the formation of carbon filaments. J Catal 131:60–73
13. Rodrigues NM, Kim MS, Baker RTK (1993) Deactivation of copper-nickel catalysts due to changes in surface composition. J Catal 140:16–29

14. Krishnankutty N, Rodriguez NM, Baker RTK (1996) Effect of copper on the decomposition of ethylene over an iron catalyst. J Catal 158:217–227

15. Chambers A, Rodriguez NM, Baker RTK (1995) Modification of the catalytic behavior of cobalt by the addition of copper. J Phys Chem 99:10581–10589

16. Leidheiser H Jr, Gwathmey AT (1948) The catalytic reaction of hydrogen and oxygen on plane faces of a single crystal of copper. J Amer Chem Soc 70:1200–1206

17. Keherer VJ Jr, Leidheiser H Jr (1954) The catalytic decomposition of carbon monoxide on large metallic single crystals. J Phys Chem 58:550–555

18. Nakagawa K, Oda H, Yamashita A, Okamoto M, Sato Y, Gamo H, Nishitani-Gamo M, Ogawa K, Ando T (2009) A novel spherical carbon. J Mater Sci 44:221–226

19. Nakagawa K, Yamagishi M, Nishimoto H, Ikenaga N, Suzuki T, Kobayashi T, M. N.-Gamo, T. Ando, (2003) Oxidized diamond as a simultaneous production medium of carbon nanomaterials and hydrogen for fuel cell. Chem. Mater. 15:4571–4575

20. Baba K, Iwasawa K, Eguchi M, Kobayashi Y, Kobori M, Nishitani-Gamo M, Ando T (2013) Interfacial nanostructure of the polymer electrolyte fuel cell catalyst layer constructed with different ionomer contents. Jpn J Appl Phys 52:06GD06-1-06GD06-5

21. Eguchi M, Baba K, Iwasawa K, Nishitani-Gamo M, Ando T (2013) The Marimo carbon as a polymer electrolyte fuel cell catalyst support. Trans Mat Res Soc Japan 38:349–352

22. Baba K, Nishitani-Gamo M, Ando T, Eguchi M (2016) Durable Marimo-like carbon support for platinum nanoparticle catalyst in polymer electrolyte fuel cell. Electrochim Acta 213:447–451

23. Ashok J, Shiva Reddy P, Raju G, Subrahmanyam M, Venugopal A (2009) Catalytic decomposition of methane to hydrogen and carbon nanofibers over Ni-Cu-SiO$_2$ catalysts. Energy Fuels 23:5–13

Publisher's Note Springer Nature remains neutral with regard to jurisdictional claims in published maps and institutional affiliations.